Levodopa-induced dyskinesia in Parkinson's disease specifically associates with dopaminergic depletion in sensorimotor-related functional subregions of the striatum

Miguel A. Labrador-Espinosa, MSc[1,2], Michel J. Grothe, PhD[1,2], Daniel Macías-García, MD[1,2], Silvia Jesús, PhD[1,2], Astrid Adarmes-Gómez, MD[1,2], Laura Muñoz-Delgado, MD[2], Paula Fernández-Rodríguez, MD[4], Juan Francisco Martín-Rodríguez, PhD[1,2,3], Ismael Huertas, PhD[1], David García Solís, MD[4], Pablo Mir, PhD[1,2].

1. Unidad de Trastornos del Movimiento, Servicio de Neurología y Neurofisiología Clínica, Instituto de Biomedicina de Sevilla, Hospital Universitario Virgen del Rocío/CSIC/Universidad de Sevilla, Seville, Spain.
2. Centro de Investigación Biomédica en Red sobre Enfermedades Neurodegenerativas (CIBERNED), Madrid, Spain.
3. Departamento de Psicología Experimental, Facultad de Psicología, Universidad de Sevilla, Sevilla, España.
4. Unidad de Medicina Nuclear, Hospital Universitario Virgen del Rocío, Sevilla, España.

***Authors for correspondence:**

Pablo Mir, email: pmir@us.es

Michel Grothe, email: mgrothe@us.es

Unidad de Trastornos del Movimiento, Instituto de Biomedicina de Sevilla (IBiS), Hospital Universitario Virgen del Rocío, Avda. Manuel Siurot s/n, 41013, Seville, Spain.

Tel.: +34 955923039; Fax: +34 955923101.

Acknowledgements

We would like to thank all the patients and their caregivers for their efforts to participate in this study. In addition to our local university hospital cohort, data used in the preparation of this manuscript were obtained from the Parkinson's Progression Markers Initiative database (www.ppmi-info.org/data). PPMI—a public-private partnership—is funded by the Michael J. Fox Foundation for Parkinson's Research. Corporate funding partners include AbbVie, Allergan, Amathus, Avid, Biogen, BioLegend, Bristol-Myers Squibb, Celgene, Denali, GE Healthcare, Genentech, GlaxoSmithKline, Janssen Neurosciene, Lilly,

Lundbeck, Merck, Meso Scale Discovery, Pfizer, Piramal, Prevail, Roche, Sanofi Genzyme, Servier, Takeda, Teva, UCB, Verily, Voyager, and philanthropic funding partner include GOLUB CAPITAL.

Conflicts of interest: None.

Sources of funding

This work was supported by the Instituto de Salud Carlos III-Fondo Europeo de Desarrollo Regional (ISCIII-FEDER) [PI14/01823, PI16/01575, PI18/01898, PI19/01576], the Consejería de Economía, Innovación, Ciencia y Empleo de la Junta de Andalucía [CVI-02526, CTS-7685], the Consejería de Salud y Bienestar Social de la Junta de Andalucía [PI-0471-2013, PE-0210-2018, PI-0459-2018, PE-0186-2019], and the Fundación Alicia Koplowitz. MALE is supported by VI-PPIT-US from the University of Seville [USE-19094-G]. MJG is supported by the "Miguel Servet" program [CP19/00031], JFM is supported by the “Sara Borrell” program [CD13/00229] and VI-PPIT-US from the University of Seville [USE-18817-A], SJ by the "Juan Rodés" program [B-0007-2019], and DMG by the “Río Hortega” program [CM18/00142].

Ethics approval

Ethical approval was granted by the Ethics Committee of Hospital Universitario Virgen del Rocío, Universidad de Sevilla, as well as the institutional review boards of the different research centres participating in the PPMI.

Consent to participate

Written informed consent was obtained from all study participants and/or authorized representatives.

Abstract

Purpose. To determine whether the development of levodopa-induced dyskinesia (LID) in Parkinson's disease (PD) specifically relates to dopaminergic depletion in sensorimotor-related subregions of the striatum.

Methods. Our primary study sample consisted of 185 locally recruited PD patients, of which 73 (40%) developed LID. Retrospective 123I-FP-CIT SPECT data was used to quantify the specific dopamine transporter (DAT) binding ratio within distinct functionally-defined striatal subregions related to limbic, executive, and sensorimotor systems. Regional DAT levels were contrasted between patients who developed LID (PD+LID) and those who did not (PD-LID) using ANCOVA models controlled for demographic and clinical features. For validation of the findings and assessment of the evolution of LID-associated DAT changes from an early disease stage, we also studied serial 123I-FP-CIT SPECT data from 343 de novo PD patients enrolled in the Parkinson Progression Marker's Initiative (PPMI) using mixed linear model analysis.

Results. Compared to PD-LID, DAT level reductions in PD+LID patients were most pronounced in the sensorimotor striatal subregion (F=5.99, p=0.016), and also significant in the executive-related subregion (F=5.30, p=0.023). In the PPMI cohort, DAT levels in PD+LID (N=161, 47%) were only significantly reduced compared to PD-LID in the sensorimotor striatal subregion (t=-2.05, p=0.041), and this difference was already present at baseline and remained largely constant over time.

Conclusion. Measuring DAT depletion in functionally-defined sensorimotor-related striatal regions-of-interest may provide a more sensitive tool to detect LID-associated dopaminergic changes at an early disease stage and could improve individual prognosis of this common clinical complication in PD.

Keywords

Dopamine transporter (DAT), Levodopa-induced dyskinesia, Parkinson's disease, FP-CIT, SPECT

Introduction

Levodopa-induced dyskinesia (LID) is one of the major motor complications related to dopaminergic treatment in patients with Parkinson's disease (PD) (1,2) and is associated with significant disability and reduced quality of life (3). LID affects approximately 40% of patients on chronic L-dopa treatment (4,5) and is characterized by involuntary, purposeless, and predominantly choreiform movements arising initially on the more affected body side (6). In terms of risk factors, high levodopa doses, duration of treatment, younger age at onset of PD, the severity of motor symptoms, and female sex, among other contributors, have been associated clinically with LID (7–9).

Although the pathophysiology of LID is still not clear, a widely discussed model hypothesizes that low intrastriatal dopamine caused by the degeneration of nigrostriatal dopaminergic projections along with high plasma and extracellular concentrations of levodopa are closely involved in the development of LID (6,10–12). The dissociation between these factors may provoke plastic changes in striatal dopaminergic neuron signalling that lead to abnormal firing patterns between the basal ganglia and the motor cortex, causing excessive disinhibition of thalamocortical neurons and overactivation of the motor cortex (13) (Figure 1).

In line with this model, neuroimaging studies could evidence a critical role of striatal dopaminergic denervation in the development of LID through molecular imaging of dopamine transporter (DAT) density using 18F-FP-CIT PET or 123I-FP-CIT SPECT. Specifically, lower DAT levels in the putamen, but not in the caudate or ventral striatum, have been shown to predict the development of LID in de novo PD patients (14). Indeed, regional striatal DAT level depletion could also predict the timing of LID onset (15), and a higher asymmetry index of the posterior putamen region has been associated with slower changes in levodopa doses (16). However, considerable controversy still exists with respect to the exact striatal subregions that are most closely involved in the development of LID. For example, a recent longitudinal imaging study found that the dopaminergic depletion involved in LID development is not limited to putaminal regions but also involves caudate areas (17). Another study found that the caudate asymmetry index, but not the putamen asymmetry index, predicted an increased risk for LID development (18). Interestingly, a recent study in *de novo* PD patients could not find significant differences in baseline DAT levels of the anterior putamen, posterior putamen, or caudate, between patients who later developed LID compared to those who did not, indicating that these rather broadly defined anatomical divisions of the striatum may not be sensitive enough to reliably detect subtle LID-associated DAT changes in this early disease stage (19).

Although the neuroanatomy of the striatum is broadly divided into the caudate nucleus, putamen, and nucleus accumbens (20,21), axonal tracing experiments in animal models have shown that specific striatal subregions related to different motor, sensory, limbic, and executive functions can be discriminated based on their distinct cortical connectivity profiles within the cortico-basal ganglia-thalamocortical loop (22–24). Accordingly, more recent *in vivo* MRI-based connectivity studies in humans could demonstrate a similar differential functional architecture of the striatum based on its region-specific cortical connectivity profiles (25,26). A study by Tziortzi et al. (27) used such striato-cortical connectivity information derived from diffusion tensor imaging to develop a regionally detailed striatal atlas in standard stereotactic space that subdivides the striatum into functional subregions based on their cortical connectivity profile. Importantly, in a subsequent pharmacologic PET imaging study, the authors could validate the functional relevance of their connectivity-based striatal atlas by demonstrating that the spatial distribution of d-amphetamine-induced dopamine release more closely corresponded to the connectivity-based functional striatal subregions as compared to the classical structural subdivisions. Based on the distinct cortical connectivity profiles, the atlas distinguishes three main functional striatal subdivisions related to limbic, executive, and sensorimotor systems, respectively, and further subdivides the sensorimotor division into three distinct subregions specifically related to rostral-motor, caudal-motor, and parietal cortical areas.

In the present study we used this detailed atlas to assess LID-associated DAT changes within functionally-defined striatal subregions. We hypothesized that the development of LID may be specifically related to DAT changes in striatal subregions that are associated with sensorimotor functions, as opposed to cognition-related subregions. In a first analysis, we studied differences in regional DAT levels between PD patients with and without LID using cross-sectional 123I-FP-CIT SPECT data from our local monocentric cohort of PD patients with varying degrees of disease evolution. For validation of the region-specific effects and assessment of the evolution of LID-associated DAT changes from an early disease stage, we also studied longitudinal 123I-FP-CIT SPECT data in relation to LID occurrence in *de novo* PD patients from the Parkinson Progression Marker's Initiative (PPMI) cohort.

Material and methods

Participants and clinical assessment

Our primary study sample was derived from a local cohort of PD patients recruited at the *Movement Disorders Unit* of the *Hospital Universitario Virgen del Rocio (HUVR)* in Seville, which is a regional reference centre

for movement disorders in southern Spain. The HUVR cohort includes PD patients who were diagnosed with idiopathic PD between 2008 and 2019 following the Movement Disorder Society Clinical Diagnostic Criteria (28). In the present study, we included 185 PD patients from this cohort based on the availability of a 123I-FP-CIT SPECT scan, which was acquired on average 2.67 ± 1.9 years after initial diagnosis and before the occurrence of LID. Over a mean available follow-up of 6.84 ± 1.82 years from initial diagnosis, 73 patients (39.5%) presented LID (PD+LID) at clinical examination and 112 patients did not (PD-LID). Disease severity was evaluated by the Hoehn and Yahr (H&Y) scale, and dopaminergic therapy was evaluated by levodopa equivalent doses (LED), LED of dopaminergic agonists, and total LED.

As an independent validation cohort, we included 343 *de novo* PD patients from the PPMI. The PPMI is a longitudinal multicentre cohort study designed to investigate the progression of clinical features as well as neuroimaging and biological markers in *de novo* PD patients as compared to healthy controls. It is a public-private partnership funded by the Michael J. Fox Foundation for Parkinson disease's research. For up-to-date information on the PPMI study, visit www.ppmi-info.org. In the present study, patients were selected from this cohort based on the availability of a 123I-FP-CIT SPECT scan at baseline and at least one follow-up visit. Longitudinal SPECT acquisitions in the PPMI study are scheduled for the first, second and fourth year study visits, and the included participant's in the present study had a median of three SPECT scans over a mean follow-up time of 1.83 ± 0.84 years. PD patients were categorized as PD+LID if they developed LID over the available clinical follow-up (6.09 ± 1.86 years), as evaluated by the respective item of the Unified Parkinson's Disease Rating Scale (UPDRS) – Part IV. This was the case for a total of 161 patients (46.9%), who developed LID on average 4.15 ± 1.83 years after study inclusion. Disease severity was evaluated by the H&Y scale and motor symptom severity by the UPDRS – Part III. Analogously to the procedures in the HUVR cohort, dopaminergic therapy was evaluated by doses of levodopa, LED by dopaminergic agonists, and total LED.

Neuroimaging acquisition

Imaging acquisition in both cohorts was performed following similar standardized imaging protocols for the acquisition of 123I-FP-CIT SPECT data.

In the HUVR cohort, SPECT data acquisition was performed on a Siemens Symbia T6 scanner with a dual-head rotating gamma camera and fan-beam collimator. Image acquisition was started between 3 and 4 h after injection

of 185 MBq of 123I-FP-CIT. A total of 120 projections of 30s each over a 360° circular orbit was acquired on a 128×128 matrix (zoom 1.23) to build the 3D images. Reconstruction was performed with the Siemens e.soft software (Siemens Healthcare, Erlangen, Germany) by filtered back-projection using a Butterworth filter.

SPECT data acquisition in the PPMI cohort was performed across multiple centers following a standardized protocol. Analogous to the HUVR cohort, the image acquisition was acquired 4 ± 0.5 hours following the injection of 111 to 185 MBq of 123I-FP-CIT. Scans were performed with a 128×128 matrix stepping of 3 degrees each for a total of 120 degrees. 3D image reconstruction was then carried out using the PMOD software (PMOD Technologies, Zurich, Switzerland). In order to improve image homogeneity across the multicentric image acquisitions, the Imaging Core Lab of the Institute for Neurodegenerative Disorders (Yale University, New Haven, Connecticut) applies standardized pre-processing steps to all SPECT acquisitions in PPMI (29). The complete standardized protocol is available at the PPMI website: http://www.ppmi-info.org/wp-content/uploads/2017/06/PPMI-TOM-V8_09-March-2017.pdf. Reconstructed 123I-FP-CIT SPECT scans were downloaded from the PPMI database in March 2018.

Neuroimaging processing

123I-FP-CIT SPECT processing was carried out in the same way for both cohorts using SPM12 (Wellcome Centre for Human Neuroimaging, Institute of Neurology, UCL, London, UK) running under MATLAB 2018a (MathWorks, Natick, MA). SPECT images were first reoriented, setting the anterior commissure as the origin of the coordinate system. Each scan was then spatially normalized into the standard stereotactic MNI (Montreal Neurological Institute) space using a 123I-FP-CIT template developed by our group (30). The resulting images were resliced to a 91x109x91 matrix of 2x2x2 mm^3 voxels. The specific 123I-FP-CIT binding ratio (SBR) was calculated for each brain voxel using the following formula: SBR = [(radioligand uptake value of voxel - mean radioligand uptake of the occipital lobe) / radioligand uptake of the occipital lobe] (31).

Functional striatal atlas and DAT quantification

DAT levels were quantified by the mean SBR in different functional subregions of the striatum as mapped in the MNI space atlas developed by Tziortzi et al (27) (Figure 2). This atlas subdivides the striatum into subregions based on their differential cortical connectivity patterns with limbic, executive, and sensorimotor areas. Thus, the limbic striatal subregion is connected with the orbital gyrus, gyrus rectus, and subcallosal gyrus/ventral anterior cingulate; the executive subregion with rostral superior and middle frontal gyri and the dorsal prefrontal cortex; and

the sensorimotor-related striatum is further subdivided into a rostral-motor subregion with connectivity to rostral area 6, pre-SMA, and the frontal eye field region; a caudal-motor subregion connected with the precentral gyrus; and a parietal subregion connected with the parietal lobe.

Statistical analysis

In the primary study, demographic and clinical characteristics of the HUVR cohort were compared between PD-LID and PD+LID groups using two-sample t-tests for parametric variables, Mann-Whitney U test for non-parametric variables and the Fisher exact test for categorical variables. Differences in subregional striatal DAT levels between PD-LID and PD+LID groups were assessed with analysis of covariance (ANCOVA) models controlled for sex, patient age at PD onset, years of disease progression at time of SPECT, H&Y stage and levodopa doses.

In the validation study, baseline demographic and clinical characteristics of the PPMI cohort were compared between PD-LID and PD+LID groups using the same statistical tests as described above for the HUVR cohort. Longitudinal changes in UPDRS-III score and dopaminergic therapy were compared between groups using linear mixed-effect modelling. Analogously, mixed-effect models of longitudinal SPECT measurements were used to investigate effects of group (PD-LID vs PD+LID), time, and the interaction between group and time on subregional striatal DAT levels. All mixed-effect models analysing subregional striatal DAT levels were controlled for sex, patient age at SPECT, UPDRS-III, and levodopa doses. For all models, group, time (in years of SPECT follow-up visit), and interaction between group and time were included as fixed effects predictors. Patient ID was included as random effect.

All statistical analyses were conducted in R version 3.5.1 and R Studio 1.2. Linear mixed-effects model analyses were carried out using the lme4 package.

Results

Demographics and clinical features of the local PD cohort

Demographics and clinical characteristics of the HUVR sample are summarized in Table 1. The mean age at onset of PD was 64.48 ± 11.03 years, and 71 patients (38.4%) were female. There were no significant differences in demographics between PD-LID and PD+LID patients, although the mean age was younger in PD+LID with trend-level statistical significance. PD+LID patients had significantly higher levodopa doses ($p < 0.001$), and higher total

LED ($p < 0.001$), but did not differ from PD-LID in LED of dopaminergic agonists. There were no significant differences between groups in any other clinical features.

Differences in DAT levels of functional striatal subregions between PD-LID and PD+LID patients in the local PD cohort

Mean DAT levels for each group in limbic, executive, whole sensorimotor, as well as rostral-motor, caudal-motor, and parietal striatal subregions are summarized in Table 2. As hypothesized, mean DAT levels in sensorimotor-related striatal subregions were significantly lower in the PD+LID group compared to the PD-LID group: whole sensorimotor ($F = 5.99$, $p = 0.016$), rostral-motor ($F = 4.51$, $p = 0.035$), caudal-motor ($F = 5.70$, $p = 0.018$) and parietal ($F = 6.73$, $p = 0.01$). Moreover, mean DAT levels in the executive-related striatal subregion were also significantly lower in PD+LID compared to PD-LID ($F = 5.30$, $p = 0.023$). Group differences in DAT levels in the limbic-related striatal subregion reached only trend-level statistical significance ($F = 3.33$, $p = 0.07$).

Demographics and clinical features of PD-LID and PD+LID patients in the PPMI cohort

Demographics and clinical characteristics of the validation cohort of *de novo* PD patients are summarized in Table 3. The mean age at onset of PD was significantly earlier in the PD+LID group compared to the PD-LID group (59.8 ± 9.4 vs 62.3 ± 9.8, $p = 0.015$). PD+LID patients also had significantly higher baseline UPDRS-III score (22.1 ± 8.3 vs 19.4 ± 9.2, $p = 0.003$) and H&Y stage (1.5 with IQR: 1-2 vs 2 with IQR: 1-2, $p = 0.033$) than PD-LID patients. There were no significant differences between groups in any other demographic or clinical features at baseline.

Longitudinal changes in motor symptoms and dopaminergic therapy of the PD+LID and PD-LID groups are illustrated in Figure 3. In mixed linear models, the UPDRS-III score was on average significantly higher in PD+LID patients compared to PD-LID patients (effect of group: $\beta = 3.14$, $t = 2.96$, $p = 0.003$). UPDRS-III score significantly increased over time in both groups (effect of time: $\beta = 2.64$, $t = 12.85$, $p < 0.001$), but this increase was less pronounced for the PD+LID group (group x time interaction: $\beta = -0.69$, $t = -2.35$, $p = 0.018$).

There was a significant group effect on levodopa doses and total LED, being significantly higher in PD+LID patients compared to PD-LID patients since first year of drug initiation (levodopa doses: $\beta = 95.19$, $t = 2.27$, $p = 0.023$; total LED: $\beta = 112.80$, $t = 2.65$, $p = 0.008$). Levodopa doses and total LED significantly increased over time in both groups (levodopa doses: $\beta = 67.10$, $t = 8.39$, $p < 0.001$; total LED: $\beta = 88.38$, $t = 10.99$, $p < 0.001$), but this increase was significantly higher in the PD+LID group compared to the PD-LID group (group x time interaction: levodopa

doses: $\beta = 32.7$, $t = 2.89$, $p = 0.004$; total LED: $\beta = 26.96$, $t = 2.37$, $p = 0.018$). LED of dopaminergic agonists was not significantly different between groups.

Differences in DAT levels of functional striatal subregions between PD-LID and PD+LID patients in the PPMI cohort

Baseline and longitudinal measurements of subregional striatal DAT measurements in the PD+LID and PD-LID groups from the PPMI cohort are summarized in Table 4 and illustrated in Figure 4. After correcting for sex, age at SPECT, UPDRS-III, and levodopa doses, DAT levels in the sensorimotor-related striatal subregion were significantly lower in PD+LID patients compared to PD-LID patients (group effect: $\beta = -0.06$, $t = -2.05$, $p = 0.041$), but no significant group effects were observed for the limbic- and executive-related striatal subregions. Among the different sensorimotor-related striatal subregions, DAT levels in rostral-motor ($\beta = -0.08$, $t = -2.14$, $p = 0.033$), and caudal-motor ($\beta = -0.06$, $t = -1.975$, $p = 0.049$) subregions were significantly lower in PD+LID than PD-LID patients, but group differences in the parietal subregion were only trend-level significant ($\beta = -0.04$, $t = -1.86$, $p = 0.064$).

DAT levels in all striatal subregions significantly decreased over time (all time effects $p < 0.001$), but longitudinal change did not differ between the PD+LID and PD-LID groups in any of the striatal subregions (all group x time interactions $p > 0.32$).

Discussion

We investigated DAT changes measured with 123I-FP-CIT SPECT within functionally-defined striatal subregions between PD patients who developed LID and those who did not. In a primary study on our local monocentric PD cohort with varying degrees of disease progression, we found that PD patients who developed LID showed significantly lower DAT levels across large parts of the striatum, and specifically in subregions associated to sensorimotor functions. The regional specificity of LID-associated DAT depletion in sensorimotor-related subregions of the striatum could be corroborated in an independent study cohort of longitudinally followed *de novo* PD patients. Interestingly, analysis of longitudinal 123I-FP-CIT SPECT data in this cohort indicated that the LID-associated differences in sensorimotor striatal DAT levels were already present at the time of initial PD diagnosis, on average 4 years before the development of LID, and group differences were largely constant over time. Together, these results indicate that the development of LID in PD is specifically related to dopaminergic denervation in striatal subregions that are associated with sensorimotor functions, and that these changes can be detected at a very early disease stage.

DAT depletion in broad anatomically-defined caudate and putaminal regions (32,33) has been related to the development of LID in PD patients in several previous studies (12,14,15,34). However, these studies had not differentiated between distinct functionally-defined striatal subregions, which may be differentially implicated in different aspects of the clinical symptomatology in PD (35–37). In agreement with previous experimental studies in animal models (38,39), our in-vivo imaging findings confirm that dopaminergic degeneration associated with the occurrence of LID specifically implicates striatal areas connected to the cortical sensorimotor system.

Furthermore, in an independent validation study using data from the PPMI cohort we found that excess DAT reductions in *de novo* PD patients who later developed LID were limited to the sensorimotor striatal region, and that this difference was already present at study baseline (coinciding with initial PD diagnosis) and remained largely constant over an average of 1.8 years of follow-up with SPECT imaging. Our results agree with previous studies that have shown the predictive role of decreased putaminal DAT levels for the development of LID in *de novo* PD patients using both the PPMI (17) and other cohorts (14,15). However, these findings contrast with other studies that could not fully reproduce this predictive effect in *de novo* PD patients (19), including a recent study using data from the PPMI cohort (18). This latter study investigated a wide range of possible risk factors for the development of LID, and although they could confirm several previously reported risk factors for LID, they did not find significant differences in baseline DAT uptake levels of the caudate or putamen between patients who did or did not develop LID. However, somewhat surprisingly, and in contrast to other studies on LID-associated DAT changes (16), the caudate asymmetry index, but not the putamen asymmetry index, was found to predict an increased risk for LID development in this study. Possible explanations for the discrepancy with our current findings on LID development in the PPMI cohort include the use of longitudinal SPECT data and its statistical modelling using mixed linear models whereas only baseline SPECT-derived DAT values were used in this previous study. However, another explanation may be that the rather broad anatomical divisions of the striatum (caudate and putamen) used in this previous study may not be sensitive enough to reliably detect subtle LID-associated DAT changes in this early disease stage (see supplemental data for a complementary analysis of standard caudate and putamen regions of interest in our data sets that corroborate this notion).

Taken together, our findings across two independent cohorts of PD patients at varying stages of disease evolution suggest that the development of LID may be specifically associated with reduced DAT levels in functionally-defined sensorimotor-related striatal subregions. These subregions are defined by their specific cortical

connectivity pattern with cortical motor areas including rostral Brodmann area 6, pre-SMA, precentral gyrus, and the frontal eye field region (27). Interestingly, recent DTI and resting-state fMRI studies have shown abnormal striato-cortical connectivity patterns in PD patients who suffer from LID, especially affecting connections between the putamen and cortical sensorimotor areas (40–42). Moreover, in a pharmacodynamic functional neuroimaging approach that mapped the effect of a single dose of levodopa on connectivity in cortico-basal ganglia motor loops, it could be shown that the dopaminergic modulation of feedback connections from the putamen to cortical motor areas was strongly involved in the development and severity of LID, but not the forward connections from cortical motor areas to the putamen (43). Our findings on specific LID-associated DAT level depletion in functional subregions of the striatum that are connected to sensorimotor cortical areas may represent a neurodegenerative correlate of this abnormal dopaminergic modulation of cortical motor areas through striatal projections. However, additional multimodal imaging studies are necessary to investigate the relation between regionally-specific DAT depletion and striato-cortical connectivity changes in the development of LID.

Although the LID-associated differences in striatal DAT levels showed highest effect size in the sensorimotor striatal subregions, it should be noted that in our primary study cohort these differences also extended into the executive striatal subregion. These results could be related to recent findings reported by Yoo et al. (44) who demonstrated that LID development was closely associated with the progression of cognitive decline, especially with frontal executive dysfunction. Interestingly, a recent multimodal 123I-FP-CIT SPECT and [^{18}F]FDG-PET imaging study found that reduced DAT levels in the cognitive part of the striatum (combined executive + limbic subregions), but not in the sensorimotor part, associated with frontomedial hypometabolism in PD patients, which likely represents a neurofunctional correlate of impaired executive functions (35). Together with our findings of a selective association of LID with DAT depletion in sensorimotor regions in drug-naïve *de novo* PD patients, this data could indicate a sequence of LID-associated DAT changes progressing from sensorimotor to executive striatal subregions with corresponding clinical-cognitive changes. Molecular neuroimaging studies over longer follow-up intervals will be necessary to study the regionally progressive neurodegenerative changes underlying LID-associated cognitive changes in more detail.

As expected, in both study cohorts we found higher doses of levodopa and total LED in PD patients who suffered LID compared to PD patients who did not develop this complication. Moreover, PD patients with LID also had more severe motor symptoms than PD patients without LID. These results are fully consistent with previous

findings on common risk factors of LID, indicating a narrowing of the therapeutic window of levodopa treatment with progression of motor symptoms in PD (45,46). Interestingly, in the PPMI cohort we also observed a higher longitudinal increase of levodopa doses in PD patients who develop LID, whereas DAT levels in the sensorimotor-related striatal subregion were already significantly reduced at baseline compared to the PD-LID group and remained relatively constant over time. This corroborates previously reported interactive effects of levodopa treatment and dopaminergic depletion on LID, where high doses of levodopa specifically associate with dyskinesia in patients with higher levels of dopaminergic depletion (47,48).

Our data suggests that the proposed method of measuring DAT depletion in a functionally-defined sensorimotor-related striatal region may provide a more sensitive imaging biomarker for detecting LID-associated dopaminergic degeneration in an early disease stage, and may thus improve the individual prognosis of, and clinical decision making for, this common medication-related complication in PD (14,15,18,49). Taking into account other known clinical risk factors, the assessment of an individual patient's LID risk through the specific measurement of sensorimotor-related striatal dopaminergic depletion at an early disease stage could help the clinician in therapeutic decision making, and potentially improve prevention and management of this complication through individually adjusted therapeutic strategies (50–52). A next step towards successful clinical translation of our current research findings to such a precision medicine approach will involve the development of accurate clinical decision support systems that integrate the information from the proposed molecular imaging biomarker with other clinical and biological sources of information within multivariate predictive models (53,54). However, it also has to be noted that our current findings were obtained in a controlled research environment and in patients from highly specialized tertiary care centers, so a further validation in less selected patient cohorts is required. Moreover, the automated analysis methods we use for measuring DAT levels in specific functionally-defined striatal subregions require expertise in computational image processing and analysis, which could pose a limitation for the implementation of this measurement in the wider healthcare system. Nevertheless, we believe that translation of this method outside of dedicated research centers will be feasible through increasingly specialized software solutions that are becoming available for medical image analysis in clinical settings (55,56). A wider clinical accessibility of our proposed regional DAT quantification method through such user-friendly software solutions will allow testing the prognostic potential of this method as a molecular imaging biomarker for increased LID risk through a diagnostic trial in a real-world clinical setting.

A principal limitation of our study is that the data from our local cohort were collected in a retrospective manner. The occurrence of LID was evaluated by clinical examination through neurologists specialized in movement disorders, but no additional standardized scales for the assessment of motor complications in PD (such as the UPDRS - Part IV or Abnormal Involuntary Movement Scale) were available, so that more detailed analyses of dyskinesia severity or type of dyskinetic complication could not be performed (48,57,58). Moreover, quantification of specific

DAT binding reductions in spatially detailed striatal subregions may benefit from partial volume correction of 123I-FP-CIT SPECT signal using anatomic information from high-resolution structural MRI (59), but this data was not available for our retrospective cohort. In general, the spatial resolution of 123I-FP-CIT SPECT scans may cast doubt on the ability of this imaging modality to discern signal from relatively small striatal subregions, particularly with respect to the distinct sensorimotor-related subdivisions defined in the employed striatal connectivity atlas (27). However, we observed reproducible differences in relation to LID-associated DAT depletion in the larger sensorimotor-related region compared to the cognition-related regions across two independent cohorts. Finally, other neuronal systems (60) and the influence of other neurotransmitters (61), such as alterations in serotonin levels (62,63), could be involved in the pathophysiology of LID, but could not be taken into account in our current study.

In summary, we provide evidence that the development of LID in PD specifically associates with dopaminergic depletion in distinct sensorimotor-related subregions of the striatum. Measuring DAT depletion in these functionally-defined regions of interest may provide a more sensitive tool to detect LID-associated dopaminergic changes in an early disease stage, and thus to improve individual prognosis of, and clinical decision making for, this common complication in PD symptomatology. Studying the relation of region-specific striatal dopaminergic denervation with functional changes in striato-cortical signaling loops, and their interaction with others pathophysiologic factors measurable by neuroimaging, such as non-dopaminergic neurotransmitter deficits or region-specific atrophic brain changes, provides an exciting venue for future research into the complex pathophysiologic mechanisms underlying LID in PD.

References

1. Poewe W, Seppi K, Tanner CM, et al. Parkinson disease. Nat Rev Dis Prim. 2017;3:1–21.
2. Marsden CD, Parkes JD. “on-Off” Effects in Patients With Parkinson’S Disease on Chronic Levodopa Therapy. Lancet. 1976;307:292–296.
3. Péchevis M, Clarke CE, Vieregge P, et al. Effects of dyskinesias in Parkinson’s disease on quality of life and health-related costs: A prospective European study. Eur J Neurol. 2005;12:956–963.
4. Ahlskog JE, Muenter MD. Frequency of levodopa-related dyskinesias and motor fluctuations as estimated from the cumulative literature. Mov Disord. 2001;16:448–458.
5. Rascol O, Brooks DJ, Korczyn AD, et al. A five-year study of the incidence of dyskinesia in patients with early Parkinson’s

disease who were treated with ropinirole or levodopa. N Engl J Med. 2000;342:1484–1491.

6. Espay AJ, Morgante F, Merola A, et al. Levodopa-induced dyskinesia in Parkinson disease: Current and evolving concepts. Ann. Neurol. 2018. page 797–811.

7. Warren Olanow C, Kieburtz K, Rascol O, et al. Factors predictive of the development of Levodopa-induced dyskinesia and wearing-off in Parkinson's disease. Mov Disord. 2013;28:1064–1071.

8. Grandas F, Galiano ML, Tabernero C. Risk factors for levodopa-induced dyskinesias in Parkinson's disease. J Neurol. 1999;246:1127–1133.

9. Fahn S, Oakes D, Shoulson I, et al. Levodopa and the progression of parkinson's disease. N Engl J Med. 2004;351:2498–2508.

10. Porras G, De Deurwaerdere P, Li Q, et al. L-dopa-induced dyskinesia: Beyond an excessive dopamine tone in the striatum. Sci Rep. 2014;4.

11. De La Fuente-Fernández R, Sossi V, Huang Z, et al. Levodopa-induced changes in synaptic dopamine levels increase with progression of Parkinson's disease: Implications for dyskinesias. Brain. 2004;127:2747–2754.

12. De La Fuente-Fernndez R, Lu JQ, Sossi V, et al. Biochemical variations in the synaptic level of dopamine precede motor fluctuations in Parkinson's disease: PET evidence of increased dopamine turnover. Ann Neurol. 2001;49:298–303.

13. Picconi B, Hernández LF, Obeso JA, et al. Motor complications in Parkinson's disease: Striatal molecular and electrophysiological mechanisms of dyskinesias. Mov Disord. 2018;33:867–876.

14. Hong JY, Oh JS, Lee I, et al. Presynaptic dopamine depletion predicts levodopa-induced dyskinesia in de novo Parkinson disease. Neurology. 2014;82:1597–1604.

15. Yoo HS, Chung SJ, Chung SJ, et al. Presynaptic dopamine depletion determines the timing of levodopa-induced dyskinesia onset in Parkinson's disease. Eur J Nucl Med Mol Imaging. European Journal of Nuclear Medicine and Molecular Imaging; 2018;45:423–431.

16. Chung SJ, Yoo HS, Lee HS, et al. The Pattern of Striatal Dopamine Depletion as a Prognostic Marker in de Novo Parkinson Disease. Clin Nucl Med. 2018;43:787–792.

17. Jeong EH, Sunwoo MK, Song YS. Serial I-123-FP-CIT SPECT Image Findings of Parkinson's Disease Patients With Levodopa-Induced Dyskinesia. Front Neurol. 2018;9:1–7.

18. Eusebi P, Romoli M, Paoletti FP, et al. Risk factors of levodopa-induced dyskinesia in Parkinson's disease: results from the PPMI cohort. npj Park Dis [Internet]. Springer US; 2018;4. Available from: http://dx.doi.org/10.1038/s41531-018-

0069-x

19. Roussakis A-A, Gennaro M, Lao-Kaim NP, et al. Dopamine Transporter Density in de novo Parkinson's Disease Does Not Relate to the Development of Levodopa-Induced Dyskinesias. J neuroinflammation Neurodegener Dis [Internet]. 2019;3:10000. Available from: http://www.ncbi.nlm.nih.gov/pubmed/31819926%0Ahttp://www.pubmedcentral.nih.gov/articlerender.fcgi?artid=PMC6901354

20. Alexander G. Parallel Organization of Functionally Segregated Circuits Linking Basal Ganglia and Cortex. Annu Rev Neurosci. 1986;9:357–381.

21. Haber SN. The primate basal ganglia: Parallel and integrative networks. J Chem Neuroanat. 2003. page 317–330.

22. Alexander GE, Crutcher MD, Delong MR. Chapter 6 Basal ganglia-thalamocortical circuits: Parallel substrates for motor, oculomotor, "prefrontal" and "limbic" functions. Prog Brain Res. 1991;85:119–146.

23. Parent A, Hazrati LN. Functional anatomy of the basal ganglia. I. The cortico-basal ganglia-thalamo-cortical loop. Brain Res. Rev. 1995. page 91–127.

24. DeLong MR, Wichmann T. Circuits and circuit disorders of the basal ganglia. Arch Neurol. 2007;64:20–24.

25. Choi EY, Thomas Yeo BT, Buckner RL. The organization of the human striatum estimated by intrinsic functional connectivity. J Neurophysiol. 2012;108:2242–2263.

26. Draganski B, Kherif F, Klöppel S, et al. Evidence for segregated and integrative connectivity patterns in the human basal ganglia. J Neurosci. 2008;28:7143–7152.

27. Tziortzi AC, Haber SN, Searle GE, et al. Connectivity-based functional analysis of dopamine release in the striatum using diffusion-weighted MRI and positron emission tomography. Cereb Cortex. 2014;24:1165–1177.

28. Postuma RB, Berg D, Stern M, et al. MDS clinical diagnostic criteria for Parkinson's disease. Mov Disord. 2015;30:1591–1601.

29. Seibyl J, Marek K, Zubal IG. The role of the core imaging laboratory in multicenter trials. Semin. Nucl. Med. 2010. page 338–346.

30. García-Gómez FJ, García-Solís D, Luis-Simón FJ, et al. Elaboration of the SPM template for the standardization of SPECT images with 123I-Ioflupane. Rev Española Med Nucl e Imagen Mol (English Ed. 2013;32:350–356.

31. Innis RB, Cunningham VJ, Delforge J, et al. Consensus nomenclature for in vivo imaging of reversibly binding radioligands. J. Cereb. Blood Flow Metab. 2007. page 1533–1539.

32. Morrish PK, Sawle G V., Brooks DJ. Regional changes in [18F]dopa metabolism in the striatum in Parkinson's disease. Brain. 1996;119:2097–2103.

33. Nandhagopal R, Kuramoto L, Schulzer M, et al. Longitudinal progression of sporadic Parkinson's disease: A multi-tracer positron emission tomography study. Brain. 2009;132:2970–2979.

34. De La Fuente-Fernández R, Pal PK, Vingerhoets FJG, et al. Evidence for impaired presynaptic dopamine function in parkinsonian patients with motor fluctuations. J Neural Transm. 2000;107:49–57.

35. Apostolova I, Lange C, Frings L, et al. Nigrostriatal Degeneration in the Cognitive Part of the Striatum in Parkinson Disease Is Associated with Frontomedial Hypometabolism. Clin Nucl Med. 2020;45:95–99.

36. Khan AR, Hiebert NM, Vo A, et al. Biomarkers of Parkinson's disease: Striatal sub-regional structural morphometry and diffusion MRI. NeuroImage Clin. 2019;21.

37. Kübler D, Schroll H, Buchert R, et al. Cognitive performance correlates with the degree of dopaminergic degeneration in the associative part of the striatum in non-demented Parkinson's patients. J Neural Transm. 2017;124:1073–1081.

38. Wong MY, Borgkvist A, Choi SJ, et al. Dopamine-dependent corticostriatal synaptic filtering regulates sensorimotor behavior. Neuroscience. 2015;290:594–607.

39. Bamford NS, Robinson S, Palmiter RD, et al. Dopamine modulates release from corticostriatal terminals. J Neurosci. 2004;24:9541–9552.

40. Herz DM, Haagensen BN, Christensen MS, et al. The acute brain response to levodopa heralds dyskinesias in Parkinson disease. Ann Neurol. 2014;75:829–836.

41. Herz DM, Haagensen BN, Nielsen SH, et al. Resting-state connectivity predicts levodopa-induced dyskinesias in Parkinson's disease. Mov Disord. 2016;31:521–529.

42. Wang L, Wang M, Si Q, et al. Altered brain structural topological properties in Parkinson's disease with levodopa-induced dyskinesias. Park Relat Disord. 2019;67:36–41.

43. Herz DM, Haagensen BN, Christensen MS, et al. Abnormal dopaminergic modulation of striato-cortical networks underlies levodopa-induced dyskinesias in humans. Brain. 2015;138:1658–1666.

44. Yoo HS, Chung SJ, Lee YH, et al. Levodopa-induced dyskinesia is closely linked to progression of frontal dysfunction in PD. Neurology. 2019;92:E1468–E1478.

45. Angela Cenci M. Presynaptic mechanisms of L-DOPA-induced dyskinesia: The findings, the debate, the therapeutic implications. Front Neurol. 2014;5:1–15.

46. Hauser RA, McDermott MP, Messing S. Factors associated with the development of motor fluctuations and dyskinesias in Parkinson disease. Arch Neurol. 2006;63:1756–1760.

47. Francardo V, Recchia A, Popovic N, et al. Impact of the lesion procedure on the profiles of motor impairment and molecular responsiveness to L-DOPA in the 6-hydroxydopamine mouse model of Parkinson's disease. Neurobiol Dis. 2011;42:327–340.

48. Putterman DB, Munhall AC, Kozell LB, et al. Evaluation of levodopa dose and magnitude of dopamine depletion as risk factors for levodopa-induced dyskinesia in a rat model of Parkinson's disease. J Pharmacol Exp Ther. 2007;323:277–284.

49. Schapira AHV. A pragmatic, personalised approach to treatment initiation in Parkinson's disease. Lancet Neurol [Internet]. Elsevier Ltd; 2020;19:376–378. Available from: http://dx.doi.org/10.1016/S1474-4422(20)30065-X

50. de Bie RMA, Clarke CE, Espay AJ, et al. Initiation of pharmacological therapy in Parkinson's disease: when, why, and how. Lancet Neurol [Internet]. Elsevier Ltd; 2020;19:452–461. Available from: http://dx.doi.org/10.1016/S1474-4422(20)30036-3

51. Fox SH, Katzenschlager R, Lim SY, et al. International Parkinson and movement disorder society evidence-based medicine review: Update on treatments for the motor symptoms of Parkinson's disease. Mov Disord. 2018;33:1248–1266.

52. Worth PF. When the going gets tough: How to select patients with Parkinson's disease for advanced therapies. Pract Neurol. 2013;13:140–152.

53. Klucken J, Kruger R, Schmidt P, et al. Management of Parkinson's disease 20 years from now: Towards digital health pathways. J. Parkinsons. Dis. 2018.

54. Zubair R, Francisco G, Rao B. Artificial intelligence for clinical decision support. Brain. 2018;102:210–211.

55. López-González FJ, Silva-Rodríguez J, Paredes-Pacheco J, et al. Intensity normalization methods in brain FDG-PET quantification. Neuroimage. 2020;222.

56. Brogley JE. DatQuant: The future of diagnosing Parkinson disease. J Nucl Med Technol. 2019;47:21–26.

57. Colosimo C, Martínez-Martín P, Fabbrini G, et al. Task force report on scales to assess dyskinesia in Parkinson's disease: Critique and recommendations. Mov. Disord. 2010. page 1131–1142.

58. Pavese N, Evans AH, Tai YF, et al. Clinical correlates of levodopa-induced dopamine release in Parkinson disease: A PET study. Neurology. 2006;67:1612–1617.

59. Trnka J, Dusek P, Samal M, et al. MRI-guided voxel-based automatic semi-quantification of dopamine transporter imaging. Phys Medica [Internet]. Elsevier; 2020;75:1–10. Available from: https://doi.org/10.1016/j.ejmp.2020.05.010

60. Calabresi P, Picconi B, Tozzi A, et al. Direct and indirect pathways of basal ganglia: A critical reappraisal. Nat Neurosci [Internet]. Nature Publishing Group; 2014;17:1022–1030. Available from: http://dx.doi.org/10.1038/nn.3743

61. Beaudoin-Gobert M, Météreau E, Duperrier S, et al. Pathophysiology of levodopa-induced dyskinesia: Insights from multimodal imaging and immunohistochemistry in non-human primates. Neuroimage. 2018;183:132–141.

62. Carta M, Carlsson T, Kirik D, et al. Dopamine released from 5-HT terminals is the cause of L-DOPA-induced dyskinesia in parkinsonian rats. Brain. 2007;130:1819–1833.

63. Roussakis AA, Politis M, Towey D, et al. Serotonin-to-dopamine transporter ratios in Parkinson disease. Neurology. 2016;86:1152–1158.

Figure legends

Figure 1. Synaptic striatocortical connections assumed to be involved in the pathophysiology of LID.

Diagram illustrating the direct (red) and indirect (blue) basal ganglia pathways and their assumed role in the pathophysiology of PD and LID. (a) In PD, the loss of dopaminergic signalling from the SNc is thought to reduce activity of the direct pathway and to increase activity of the indirect pathway, which together leads to excessive activation of the (inhibitory) output nuclei (GPi/SNr). This in turn results in overinhibition (thick red lines) of thalamic-cortical neurons and consequent suppression of movement. (b) By contrast, LID is assumed to stem from an excessive dopaminergic stimulation specifically of the direct pathway (thick red lines), which leads to increased inhibition of the output nuclei (GPi/SNr) and thus an abnormal overactivation of thalamo-cortical neurons. Adapted from (13). Arrow heads indicate excitatory connections, perpendicular endings indicate inhibitory connections. Abbreviations: SNc = substantia nigra pars compacta; SNr = substantia nigra pars reticulata; GPe = globus pallidus pars externa; GPi = globus pallidus pars interna; STN = subthalamic nucleus.

Figure 2. Functional striatal subregions and DAT quantification.

(a) Anatomical illustration of the employed atlas of functional striatal subdivisions (27) overlaid on representative coronal (top row) and axial (bottom row) sections of a high-resolution MRI template in MNI space. Numbers indicate the respective MNI space coordinates. Colors refer to the different subregions: blue = limbic; green = executive; orange = sensorimotor. (b) A representation of this atlas in an individual preprocessed 123I-FP-CIT SPECT scan used for automated DAT quantification in the different functional subdivisions.

Figure 3. Longitudinal changes in UPDRS-III scores and levodopa equivalent doses for PD+LID and PD-LID groups in the PPMI cohort.

(a) Longitudinal levodopa equivalent doses and (b) Total UPDRS-III score over follow-up time illustrated by the mean value and standard error for each visit. Levodopa doses were significantly higher in PD+LID patients compared to PD-LID patients since first year of drug initiation, and the dosage increase over time was significantly higher in PD+LID patients. The UPDRS-III score was on average significantly higher in PD+LID patients compared to PD-LID patients, although the UPDRS-III score increase over time was less pronounced for the PD+LID group. Abbreviation: PD-LID = PD patient group who did not develop LID; PD+LID = PD patient group who developed LID; BL = baseline visit.

Figure 4. Longitudinal DAT binding changes in striatal subregions for PD+LID and PD-LID groups in the PPMI cohort.

DAT changes in the (a) limbic, (b) executive, and (c) sensorimotor striatal region over follow-up time illustrated by the mean value and standard error for each visit. DAT levels in the sensorimotor-related striatal subregion were significantly lower in PD+LID patients compared to PD-LID patients, but no significant differences were observed for the limbic- and executive-related striatal subregions. Abbreviation: PD-LID = PD patient group who did not develop LID; PD+LID = PD patient group who developed LID; BL = baseline visit.

Figure 1

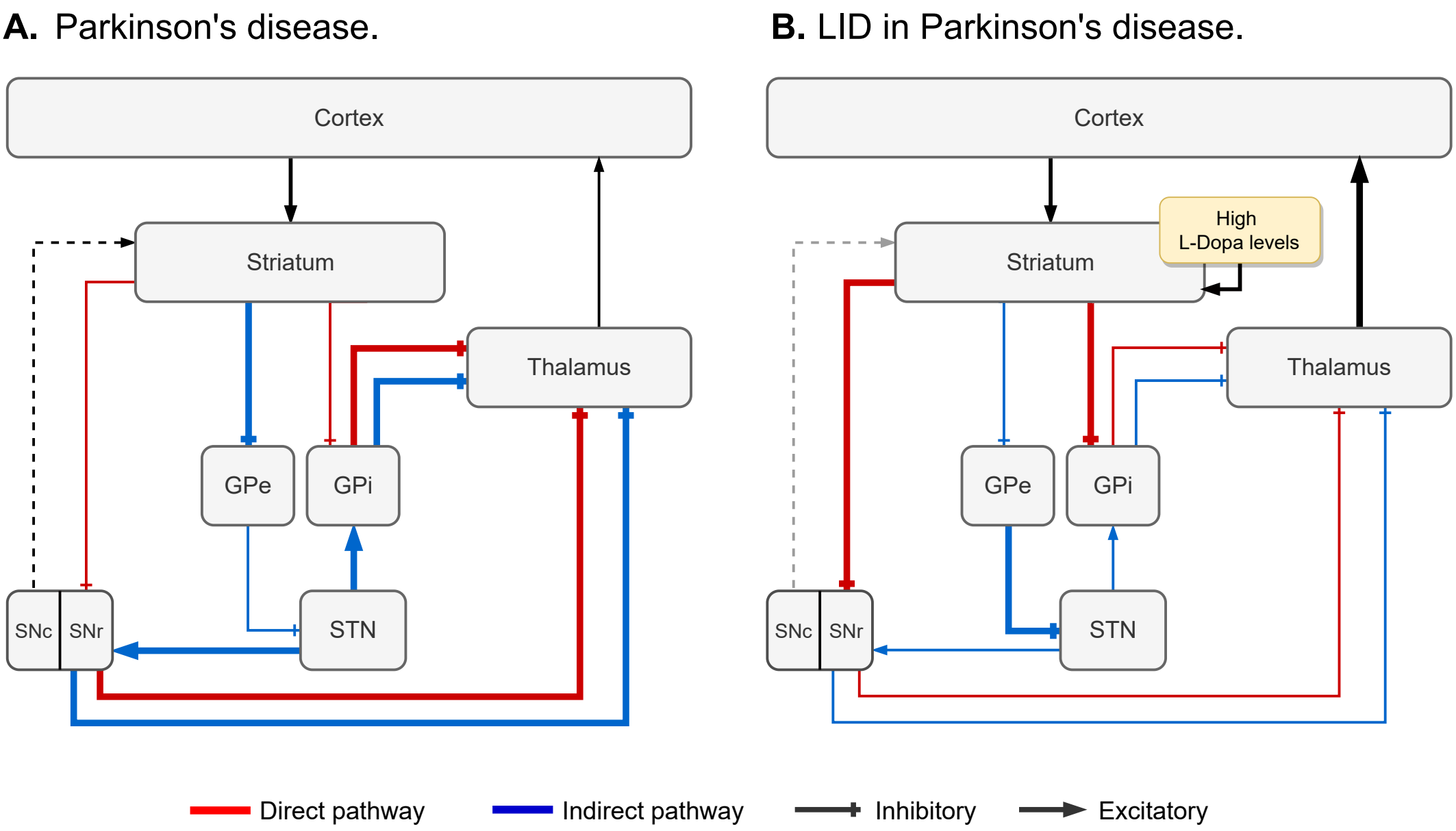
A. Parkinson's disease.
B. LID in Parkinson's disease.
Cortex
Striatum
Thalamus
GPe
GPi
SNc
SNr
STN
High
L-Dopa levels
Direct pathway
Indirect pathway
Inhibitory
Excitatory

Figure 2

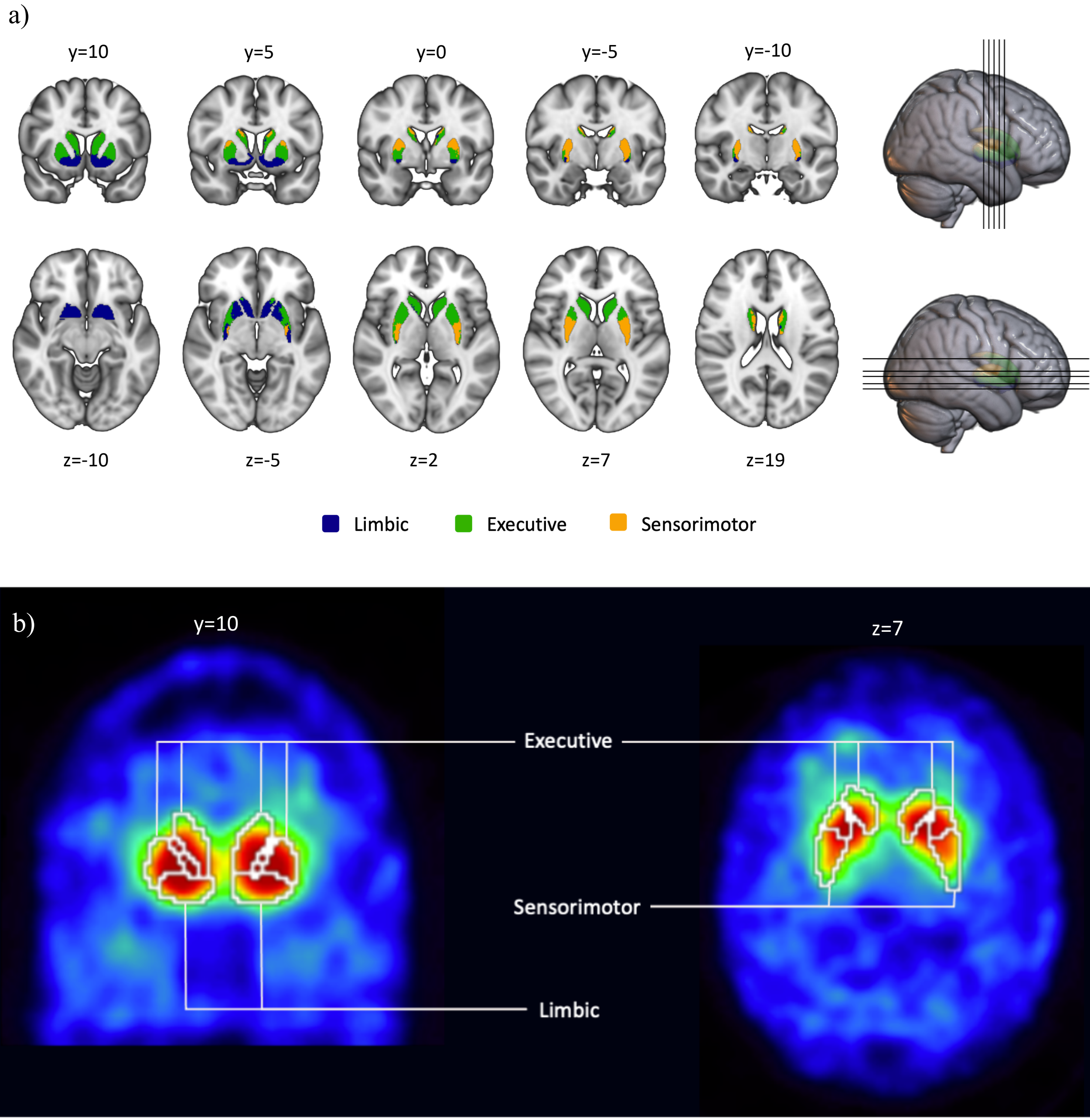
a)
y=10
y=5
y=0
y=-5
y=-10
z=-10
z=-5
z=2
z=7
z=19
Limbic
Executive
Sensorimotor
b)
y=10
z=7
Executive
Sensorimotor
Limbic

Figure 3

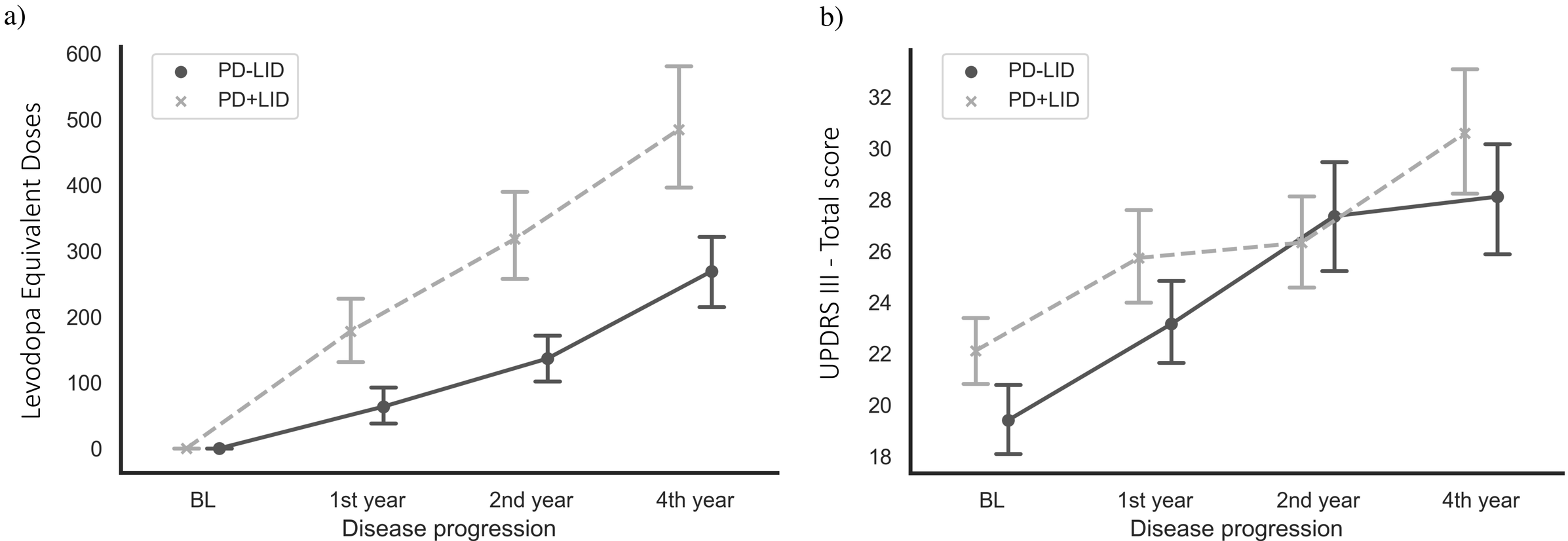
a)
600
500
400
300
200
100
0
Levodopa Equivalent Doses
PD-LID
PD+LID
BL
1st year
2nd year
4th year
Disease progression
b)
32
30
28
26
24
22
20
18
UPDRS III - Total score
PD-LID
PD+LID
BL
1st year
2nd year
4th year
Disease progression

Figure 4

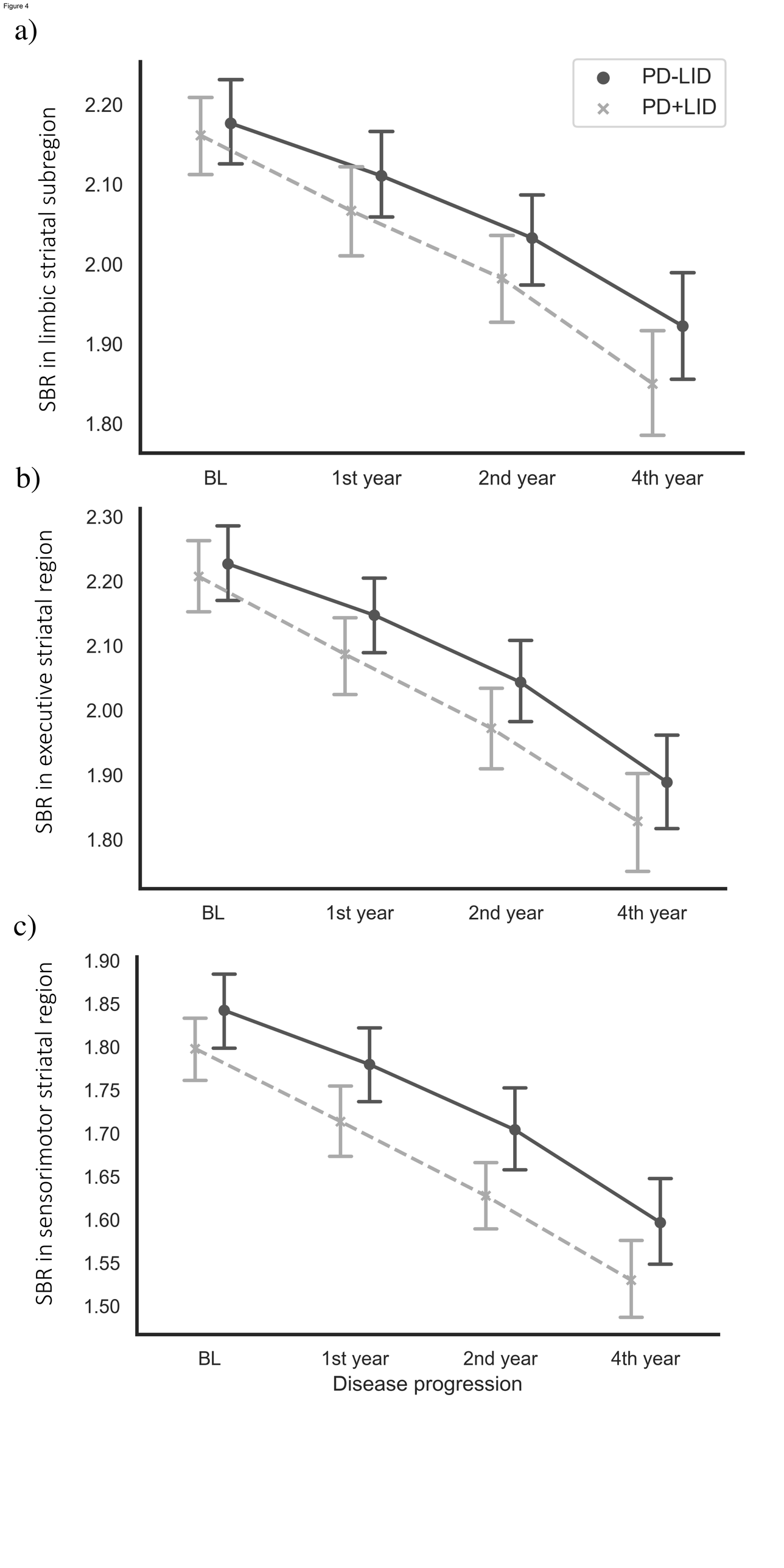
a)
PD-LID
PD+LID
SBR in limbic striatal subregion
2.20
2.10
2.00
1.90
1.80
BL
1st year
2nd year
4th year
b)
SBR in executive striatal region
2.30
2.20
2.10
2.00
1.90
1.80
BL
1st year
2nd year
4th year
c)
SBR in sensorimotor striatal region
1.90
1.85
1.80
1.75
1.70
1.65
1.60
1.55
1.50
BL
1st year
2nd year
4th year
Disease progression

Table 1. Demographics and clinical characteristics of the local PD cohort

Variables	PD-LID ($n = 112$)	PD+LID ($n = 73$)	Stats (p value)
Gender, N (%) Female	40 (36 %)	31 (42 %)	$\chi^2 = 0.59$ (0.443)
Age	65.6 ± 11.35	62.76 ± 10.37	$t = 1.75$ (0.081)
Age at disease onset	58.6 ± 11.24	56.16 ± 10.63	$t = 1.48$ (0.139)
Disease duration (years)	7.00 ± 1.37	6.59 ± 2.35	$t = 1.33$ (0.186)
Disease duration at SPECT (years)	2.75 ± 1.81	2.57 ± 2.03	$t = 0.64$ (0.524)
Hoehn & Yahr stage	2 (2 – 2.5)	2 (2 – 2)	$U = 3492$ (0.07)
Levodopa doses	619.48 ± 338.05	946.3 ± 395.19	$t = -5.6$ (<0.001)
LEDD by agonists	266.89 ± 121.92	306.88 ± 146.72	$t = -1.46$ (0.127)
Total LEDD	619.48 ± 338.05	891.65 ± 470	$t = -4.00$ (<0.001)

The descriptive values presented are number (%) for female sex, median (IQR) for Hoehn & Yahr stage, and mean ± standard deviation for all other continuous variables.

Abbreviation: PD-LID = PD patient group who did not develop LID; PD+LID = PD patient group who developed LID; LEDD = Total levodopa equivalent doses.

Table 2. Mean regional striatal DAT binding in the local PD cohort

Striatal subregions	PD-LID ($n = 112$)	PD+LID ($n = 73$)	Cohen's *d*	F value (*p* value)
Limbic	2.19 ± 0.34	2.1 ± 0.3	0.27	*F* = 3.33 (0.07)
Executive	2.22 ± 0.42	2.1 ± 0.36	0.31	*F* = 5.30 (0.023)
Sensorimotor	1.86 ± 0.33	1.74 ± 0.26	0.38	*F* = 5.99 (0.016)
Rostral motor	2.12 ± 0.42	1.99 ± 0.35	0.33	*F* = 4.51 (0.035)
Caudal motor	1.85 ± 0.33	1.73 ± 0.26	0.38	*F* = 5.70 (0.018)
Parietal	1.66 ± 0.28	1.55 ± 0.22	0.41	*F* = 6.73 (0.01)

The descriptive values presented are mean specific binding ratio (SBR) ± standard deviation, the Cohen's *d* effect size for (unadjusted) group differences between PD-LID and PD+LID, and ANCOVA stats.

Abbreviation: PD-LID = PD patient group who did not develop LID; PD+LID = PD patient group who developed LID;

Table 3

Table 3. Demographics and clinical characteristics of the PPMI cohort

Variables	PD-LID ($n = 182$)				PD+LID ($n = 161$)			
	BL	1st Visit	2nd Visit	4th Visit	BL	1st Visit	2nd Visit	4th Visit
Gender	64 (35%)	-	-	-	53 (33%)	-	-	-
Age	62.87 (9.93)	63.57 (10.05)	64.78 (10.2)	67.20 (10.23)	60.25 (9.45)	61.26 (9.34)	62.84 (9.49)	65.09 (8.90)
Disease duration years	0.57 (0.55)	1.73 (0.61)	2.65 (0.53)	4.6 (0.55)	0.49 (0.5)	1.57 (0.52)	2.58 (0.55)	4.61 (0.53)
UPDRS III	19.37 (9.15)	23.15 (10.04)	27.35 (11.81)	28.11 (10.6)	22.11 (8.25)	25.73 (10.51)	26.32 (9.87)	30.59 (10.84)
Levodopa doses	-	63.49 (165.27)	136.52 (224.29)	269.18 (269.58)	-	177.86 (306.56)	318.04 (391.34)	484.31 (450.16)
Dopamine agonist LEDD	-	46.46 (85.2)	74.44 (117.1)	89.46 (116.88)	-	44.95 (85.12)	66.17 (116.71)	84.14 (136.52)
Total LEDD	-	153.36 (189.18)	273.88 (231.13)	430.57 (265.7)	-	268.68 (303.04)	461.01 (392.23)	634.49 (454.18)

The descriptive values presented are number (%) for female sex and mean (standard deviation) for all other continuous variables.

Abbreviation: PD-LID = PD patient group who did not develop LID; PD+LID = PD patient group who developed LID; BL = baseline visit; LEDD = Total levodopa equivalent doses; UPDSR III = Unified Parkinson's Disease Rating Scale – "Part III" score.

Table 4

Table 4. Mean regional striatal DAT binding in serial SPECT data from the PPMI cohort

Striatal subregions	Descriptive values					Mixed-linear model stats
	Group	BL	1st Visit	2nd Visit	4th Visit	(Beta, t value, p value)
Limbic	PD-LID	2.19 (0.37)	2.12 (0.34)	2.05 (0.36)	1.93 (0.33)	a. β = -0.03, t = -0.84, p = 0.40 b. β = -0.05, t = -7.38, p < 0.001
	PD+LID	2.18 (0.33)	2.08 (0.36)	1.99 (0.34)	1.86 (0.32)	c. β = -0.004, t = -0.53, p = 0.60
Executive	PD-LID	2.23 (0.39)	2.15 (0.36)	2.04 (0.39)	1.89 (0.35)	a. β = -0.05, t = -1.23, p = 0.22 b. β = -0.07, t = -9.38, p < 0.001
	PD+LID	2.21 (0.36)	2.09 (0.39)	1.97 (0.37)	1.83 (0.36)	c. β = -0.0004, t = -0.05, p = 0.96
Sensorimotor	PD-LID	1.84 (0.29)	1.78 (0.27)	1.70 (0.29)	1.60 (0.25)	a. β = -0.06, t = -2.05, p = 0.041 b. β = -0.05, t = -10.27, p < 0.001
	PD+LID	1.80 (0.25)	1.71 (0.25)	1.63 (0.24)	1.53 (0.23)	c. β = 0.005, t = 0.77, p = 0.44
Rostral motor	PD-LID	2.13 (0.37)	2.03 (0.35)	1.93 (0.37)	1.81 (0.33)	a. β = -0.08, t = -2.14, p = 0.033 b. β = -0.07, t = -10.96, p < 0.001
	PD+LID	2.05 (0.33)	1.95 (0.33)	1.83 (0.32)	1.70 (0.32)	c. β = 0.005, t = 0.57, p = 0.57
Caudal motor	PD-LID	1.82 (0.29)	1.77 (0.27)	1.69 (0.30)	1.58 (0.26)	a. β = -0.06, t = -1.975, p = 0.049 b. β = -0.05, t = -9.53, p < 0.001
	PD+LID	1.78 (0.25)	1.69 (0.25)	1.61 (0.25)	1.51 (0.23)	c. β = 0.01, t = 0.74, p = 0.46
Parietal	PD-LID	1.64 (0.23)	1.59 (0.21)	1.54 (0.24)	1.45 (0.20)	a. β = -0.04, t = -1.86, p = 0.064 b. β = -0.04, t = -8.70, p < 0.001
	PD+LID	1.61 (0.20)	1.55 (0.21)	1.48 (0.20)	1.41 (0.17)	c. β = 0.0, t = 0.99, p = 0.32

The descriptive values presented are mean specific binding ratio (SBR) (standard deviation). Mixed-linear model stats are a) group effect, b) time effect, and the c) group x time interaction.

Abbreviation: PD-LID = PD patient group who did not develop LID; PD+LID = PD patient group who developed LID; BL = baseline visit

Supplementary data.

Complementary analysis of specific [^{123}I]-FP-CIT binding ratio in standard anatomically-defined caudate and putamen regions.

In this complementary analysis, dopamine transporter (DAT) levels were quantified by the mean specific binding ratio (SBR) of [^{123}I]-FP-CIT in standard anatomically-defined caudate and putamen regions (1). The same methodology of the main study to compare DAT levels between groups (ANCOVA for local cohort and linear-mixed model for PPMI cohort) was used. The local cohort results showed that mean DAT levels in the putamen region were significantly lower in the PD+LID group compared to the PD-LID group, whereas group differences in DAT levels in the caudate region reached only trend-level statistical significance (supplementary table 1). However, in the PPMI cohort no significant group effects were observed for any of these two regions (supplementary table 2).

1. Tziortzi AC, Searle GE, Tzimopoulou S, Salinas C, Beaver JD, Jenkinson M, et al. Imaging dopamine receptors in humans with [11C]-(+)-PHNO: Dissection of D3 signal and anatomy. Neuroimage. 2011;

Supplementary Table 1. Mean DAT binding in standard anatomical striatal regions for each group in HUVR cohort.

Striatal regions	PD-LID ($n = 112$)	PD+LID ($n = 73$)	Stats (F value, p value)
Caudate	1.01 ± 0.35	0.95 ± 0.32	$F = 3.27$, $p = 0.07$
Putamen	1.19 ± 0.41	1.04 ± 0.34	$F = 6.30$, $p = 0.01$

The descriptive values presented are mean specific binding ratio (SBR) (standard deviation).

Abbreviation: PD-LID = PD patient group who did not develop LID; PD+LID = PD patient group who developed LID;

Supplementary Table 2. Mean striatal DAT in connectivity-based functional regions for each group in longitudinal cohort.

Striatal subregions	PD-LID ($n = 182$)				PD+LID ($n = 161$)				Stats (Beta, *t* value, *P* value)
	BL	1st Visit	2nd Visit	4th Visit	BL	1st Visit	2nd Visit	4th Visit	a. Group effect. b. Time effect. c. Group x time interaction.
Caudate	2.00 (0.34)	1.94 (0.31)	1.86 (0.34)	1.73 (0.31)	2.00 (0.32)	1.91 (0.35)	1.80 (0.33)	1.69 (0.32)	a. β = -0.03, t = -1.03, p = 0.30 b. β = -0.05, t = -7.75, $p < 0.001$ c. β = -0.0008, t = 0.11, p = 0.91
Putamen	2.19 (0.37)	2.11 (0.35)	2.01 (0.37)	1.87 (0.33)	2.15 (0.33)	2.03 (0.35)	1.93 (0.34)	1.79 (0.32)	a. β = -0.05, t = -1.47, p = 0.14 b. β = -0.07, t = -10.33, $p < 0.001$ c. β = 0.0001, t = -0.02, p = 0.99

The descriptive values presented are mean specific binding ratio (SBR) (standard deviation). Mixed-linear model stats are a) group effect, b) time effect, and the c) group x time interaction.

Abbreviation: PD-LID = PD patient group who did not develop LID; PD+LID = PD patient group who developed LID;